International Journal of Mechanical and Production Engineering Research and Development (IJMPERD)
ISSN (P): 2249-6890; ISSN (E): 2249-8001
Vol. 7, Issue 6, Dec 2017, 429-436

EFFECT OF FRICTION STIR WELDING PROCESSON MECHANICAL PROPERTIESAND MICROSTRUCTURE OF ZE42 MAGNESIUM ALLOY

A. K. DARWINS[1] & M. SATHEESH[2]

[1]*Research Scholar, Department of Mechanical Engineering, Noorul Islam University, Kumaracoil, Tamilnadu, India*

[2]*Assistant Professor, Department of Mechanical Engineering, Noorul Islam University, Kumaracoil, Tamilnadu, India*

ABSTRACT

A new series of magnesium alloys are being developed as due to good properties with any rare earth components. In order to investigate the effects of friction stir welding (FSW) on microstructures and thermo gravimetric analysis of ZE42 magnesium alloy, the hot-extruded alloy plates were butt welded by FSW at various welding speeds. The results showed that the alloy was jointed without defects. The alloy is characterized by mechanical properties, SEM, XRD, TGA and FTIR. With increasing welding speed, the maximum intensity in the NZ first decreased and then increased. In all cases the tensile properties of the alloy after FSW decreased due to the softened region at the heat-affected zone (HAZ), FT-IR results helps in distinguishing strong absorption appear in the region of nugget zone it is easily recognized by bands.

KEYWORDS: Magnesium Alloy, Microstructure, Hardness XRD & EDAX

Received: Oct 24, 2017; **Accepted:** Nov 15, 2017; **Published:** Nov 27, 2017; **Paper Id.:** IJMPERDDEC201749

Original Article

INTRODUCTION

ZE42 series of magnesium alloys have gained increasing interest due to high mechanical properties with any rare earth components, which are promising for commercial applications in automobile, aerospace, transport and other fields, as described [1]. The microstructure evolution and thermal analysis of Mg alloy sheet particles and found the alloy had good tensile properties at various temperatures [2, 3]. The compositional optimization of ZE42 alloys for higher age hardening response. Discharge behavior and electrochemical properties of Mg–Al–Sn alloy anode. However, relatively little attention has been remunerated to the welding process of Mg-Al-Sn alloys [4]. In fact, a reliable welding process is essential, for commercial application of Mg-Al-Sn alloys. Friction stir welding (FSW) is a green solid-state joining technology, which can eliminate the welding problems normally associated with traditional fusion welding technologies [5]. The effect of tapered tool pin profile on microstructure and mechanical properties of friction stir welded AZ42magnesium alloy [6]. Author revealed about influence of micro structural changes and induced residual stresses on tensile properties of AZ31magnesium alloy joints after FSW [7]. The multi-response optimization of process parameters for friction stir welded AM20 magnesium alloy by Taguchi grey relational analysis. And rare-earth containing ZEK120 magnesium alloy sheets were successfully joined using friction stir spot welding [8]. While there are only some limited studies on the friction stirweldedmg-ZE42 alloys. In a previous study we reported that Mg alloys were successfully welded by FSW [9]. However, there is no experimental work available on the changes of microstructure, DSC, FT-IR and mechanical properties of ZE42 alloys after FSW at various welding speeds. Therefore, this work focuses primarily on the effects of FSW on microstructure, XRD, FT-IR, thermo gravimetric and mechanical properties of Mg-ZE42 alloy with different

welding speeds, where particular attention was paid to investigate the relationship between microstructure and mechanical properties of Mg-5Al-3Sn magnesium alloy after FSW.

MATERIALS AND METHODS

The base materials were Mg-ZE42 plates with dimensions of 120 mm (length) × 50 mm (width) × 6 mm (thickness). A simple FSW tool made from H13 steel was used with a tapered tool pin 5 mm in diameter and 3.7 mm in length. After being rigidly held the base materials in position on the anvil, butt FSW process was conducted along the extruding direction at a shoulder plunge depth of 0.15 mm, which was being set FSW machine, with a tool tilt angle of 2.5°. Through a large number of pre-experiments, it was found that rotation rate should be preferably 1050 rpm to achieve defect free weld joints with excellent appearance and mechanical properties by FSW, when welding speed was in a certain range [10, 11]. So the constant rotation rate was 1050 rpm. To investigate the microstructure and mechanical properties of Mg-ZE42 magnesium alloy after FSW at various welding speeds, three different welding speeds were used in this study. The schematic diagram of ZE42 Mg alloy plates used for FSW is shown in Fig 1.

Figure 1: The Schematic diagram of ZE42 Mg Alloy Plates used for FSW

The joints after FSW were examined by X-ray radiography and the thermo gravimetric analysis was performed on the cross section of the welds perpendicular to the welding direction [12]. After being mechanically ground without polishing, the weld cross-sections were chemically etched with a mixture of 5 ml acetic acid, 120 ml ethanol, 5 g picric acid, and 10 ml distilled water. Microstructures of the joints were observed by an optical microscope and a scanning electron microscope (SEM) at 20 Kv with INCA Energy 350 energy-dispersive X-ray spectroscopy (EDS) analysis system. After been broken into small pieces and put into the crucible, thermal analysis of the samples was carried out at a heating rate of 10 °C/min and an argon flow rate of 50 ml/min by using differential scanning calorimetric. After the samples were ground using silicon papers, phase composition and crystallographic texture distribution from the top surface of the samples were tested by X-ray diffractometer (XRD), using Cu Kα radiation at 60 kV and 30 mA with a sample tilt angle ranging from 10 to 90°. Hardness at transverse direction was measured across the joint center, along the mid-thickness every 1 mm spacing with a 120 g load for 10 s on MH-3 Vickers hardness tester. Transverse tensile test samples were cut perpendicularly to the extruding direction for the BM and the weld joints before and after annealing, and the welded region was centered, within the 50 mm gauge length, in accordance with ASTM standard [13, 14]. Tensile tests were carried out on CMT-5105 mechanical tester with a crosshead speed of 0.5 mm/min at room temperature. The results of tensile tests were taken from three specimens to ensure the accuracy and reliability of experimental results.

RESULTS AND DISCUSSIONS

MECHANICAL PROPERTIES

Vickers hardness distribution across the joint center, measured along the mid-thickness is shown in Fig. 2. The

hardness of the BM was in the range of 60–73 HV. It is found that the hardness distribution profiles exhibited after FSW. The hardness profiles had little variation with increasing welding speed. The lowest hardness values were observed in the HAZ at AS regardless of welding speed [15]. The ultimate tensile strength (UTS), yield strength (YS) and elongation of the BM was determined to be about 170MPa, 167MPa and 14% respectively is shown in Fig.3. It is noted that the elastic behavior (i.e. the Young's modulus) of the BM vs. weld joints was different [16]. It is seen that after FSW both the strength and elongation decreased without regard to welding speed, especially the elongation. It is also found that both UTS and YS increased with increasing welding speed, while the increasing degree of UTS was not as obvious as that of YS. The elongation of the joints after FSW had no obvious changes with increasing welding speed. The typical SEM micrographs of tensile fracture surfaces for the BM and the 120 mm/min joint are shown in Fig. 4. For the BM, the tensile fracture is composed of elongated dimples accompanied by some tear ridges, as shown in Fig. Also, the dimple-like characteristics is shown on the fracture surface of the weld joints after FSW.

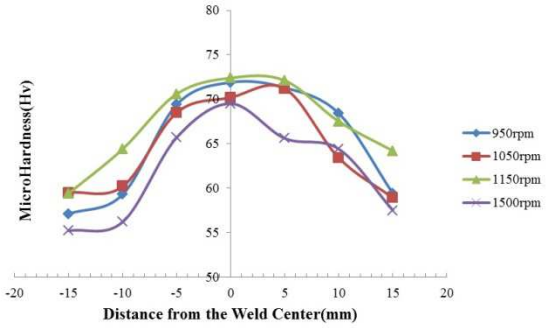

Figure 2: Hardness Properties of FSW Processed ZE42 Mg Alloy

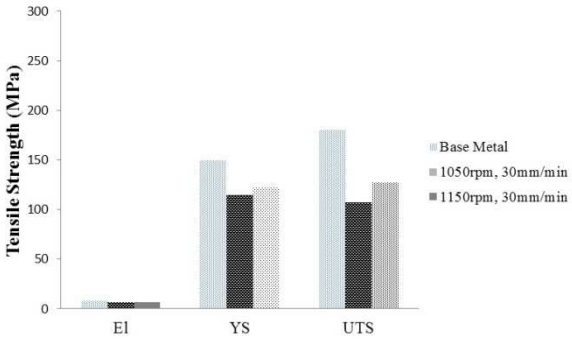

Figure 3: Histogram Image of Tensile Properties of the ZE42 Magnesium Alloy

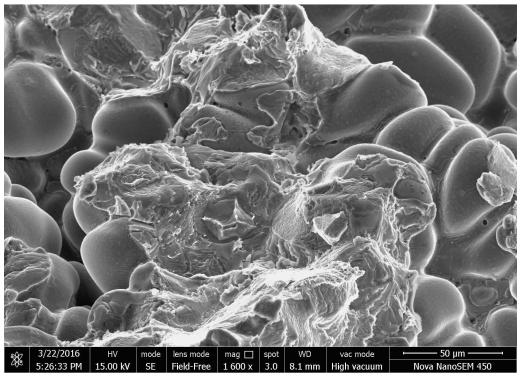

Figure 4: SEM Photographs of Tensile Fracture of 120 mm/min-Joint FSW

MICROSTRUCTURE

The SEM microstructures at different zones in the cross-section of the typical joints are shown in Fig. 5. The XRD and EDAX analysis of the mg alloy is shown in Fig. 6 and Fig.7 respectively. Fig.6 shows the XRD analysis of the NZ in the joints after FSW [17]. It is found that high peaks are found with increasing welding speed at a constant rotation rate of 1050 rpm, the grain size of Mg matrix decreased, while some intermetallic particles Zn scratched at the high welding speed of 120mm/min. It reveals that, ZE42 mg phase was dissolved, while base alloy phase remained in the NZ of the welds after FSW, which was consistent with the XRD and SEM analysis [18].

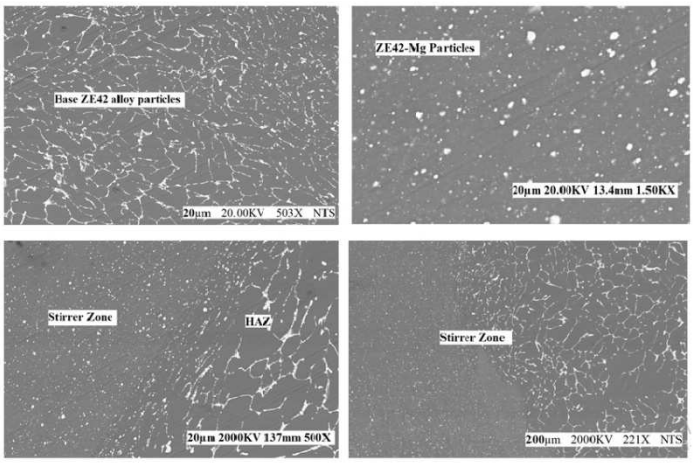

Figure 5: SEM Micrographs of ZE42at Different FSW Speeds

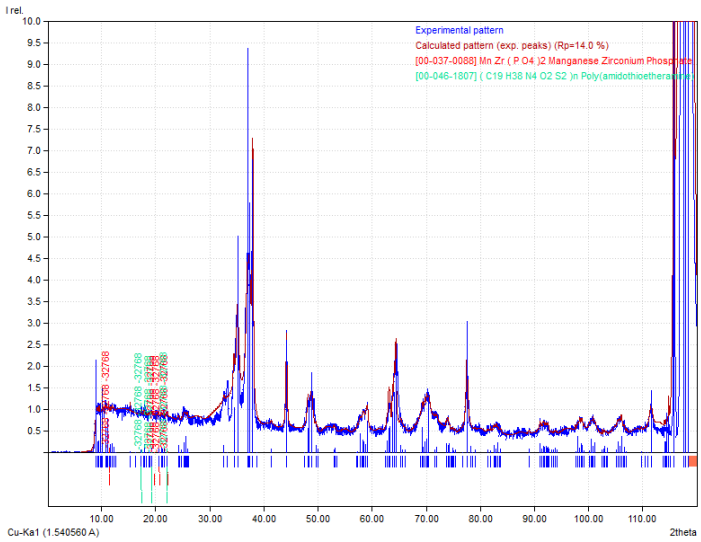

Figure 6: XRD Analysis of NZ in the Joints after FSW at 120mm/min Welding Speed

THERMAL ANALYSIS

It is found that the peak temperature reached during friction stir processing varied between 600 °C and 650 °C with translational speeds of 20–30 in/min at a constant rotation rate of 1050 rpm, and the peak temperature increased with increasing of the rotation rate. The welding temperature of the commercial ZE42 mg alloy during FSW was about 648 °C at 950 rpm and 200mm/min is shown in Fig.8. Therefore, there are reasons to believe that the maximum temperature during FSW will not exceed 600 °C with the process parameters in the present study. While Mg-Zn phase is with good

thermal stability, and its dissolution point is much higher than the temperature of 600°C [19]. So the Mg-Zn phase with better thermal stability can be retained in the NZ after FSW. The warm strength of Mg-ZE42 is higher than that of base metal. Hence, as the % of alloy in the composition expands its introduction of start temperature increments or gets fortified [20].

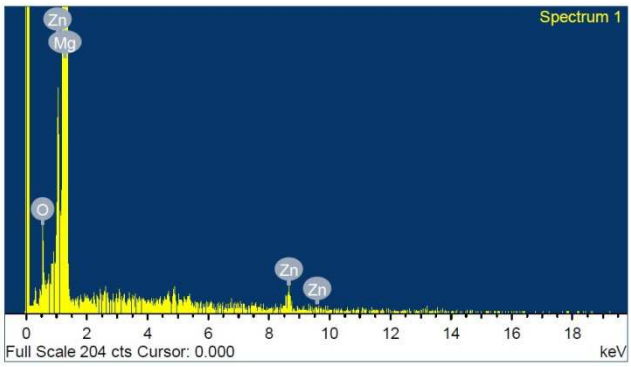

Figure 7: EDAX Analysis of NZ in the Joints after FSW at 120mm/min Welding Speed

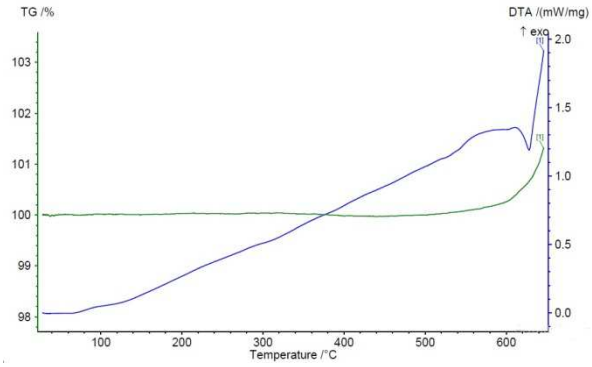

Figure 8: DSC Heating Temperature Curves of the NZ in the 120 mm/min-Joint

This is because the HAZ is heated sufficiently without plastic deformation of original grains during FSW with recovery of cold work and coarsening of precipitates. The grains in the TMAZ are with certain orientation in the direction of the metal-flow due to the stirring during FSW.

FOURIER TRANSFORM INFRARED SPECTRUM

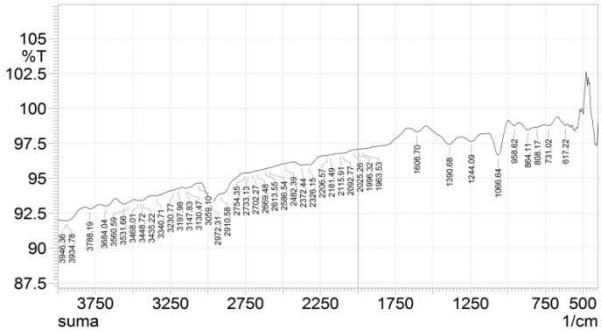

Figure 9: FTIR Result of the FSW Processed NZ in the 120mm/min-Joint

Fourier Transform Infra – Red is just passing infra-red radiation will give a quick and qualitative indication about the change in the chemical structure. The spectra of ZE42 FSW processed are shown in Fig.9. The broad adsorption band

in the region around 3120cm^{-1} would be alkane residues, are detected from C-H stretching and C-H deformation absorptions [21]. C-H stretching absorption bands appear just below 3000 cm^{-1} one for symmetrical and other for asymmetrical vibrations.

CONCLUSIONS

In the present work ZE42 magnesium alloy is friction stir welded with welding speeds ranging from 120 to 120 mm/min at a constant rotation rate of 1050 rpm, and the effects of friction stir welding (FSW) on microstructure, XRD, EDAX, DSC, FTIR, hardness and tensile properties of magnesiumalloyMg-ZE42 were investigated. The main conclusions are as follows.

- Mg-ZE42 magnesium alloy was jointed without defects at various welding speeds by FSW process. The welded joint produced at 120mm/min gave a maximum ultimate tensile strength (UTS) of 169MPa. In all cases the tensile strength of the joints after FSW was lower than the BM strength, which was induced by the dissolution of phases in the nugget zone (NZ), the softened region at the heat-affected zone (HAZ) caused by grain growth, the residual stress and dislocation content in the TMAZ.
- With increasing welding speed, the increasing degree of the UTS of joints after FSW was not as obvious as that of the yield strength (YS) because the effect of welding speed on the YS was much heavier than on the UTS.
- EDS and XRD studies make sure the availability of mg and Zn alloy particles in the peak, with compounds has been found in the alloy. SEM images represents welding speed zone elements are uniformly dispersed and the particles are interfaces each other is determined.
- TGA/DTA shows that the increase in % of alloy inflated the ignition amount. FTIR intensity is regarding 3120.42cm^{-1} band shows the high attraction absorption indicates within the chemical structure of the heat affected zone at maximum rotational speed.

REFERENCES

1. *K. Hono, C. L. Mendis, T. T. Sasaki, K. Ohishi, Towards the development of heat-treatable high-strength wrought Mg alloys, Scr. Materials.2010; 63: 710–715.*
2. *D. Luo, H. Y. Wang, L. Zhang, G. J. Liu, J. B. Li, Q. C. Jiang, Microstructure evolution and tensile properties of hot rolled Mg-6Al-3Sn alloy sheet at elevated temperatures, Materials Science Engineering A.2015;643: 149–155.*
3. *J. She, F. S. Pan, J. Zhang, A. T. Tang, S. Q. Luo, Z. W. Yu, Microstructure and mechanical properties of Mg-Al-Sn extruded alloy, Journal of Alloys and Compounds.2016; 657:893–905.*
4. *K. Yu, H. Q. Xiong, L. Wen, Y. L. Dai, S. H. Yang, S. F. Fan, et al., Discharge behavior and electrochemical properties of Mg–Al–Sn alloy anode for seawater activated battery, Trans. Nonferrous Metals Soc. China.2015; 25: 1234–1240.*
5. *P. Motalleb-nejad, T. Saeid, A. Heidarzadeh, K. H. Darzi, M. Ashjari, Effect of tool pin profile on microstructure and mechanical properties of friction stir welded AZ31B magnesium alloy, Materials and Design. 2014; 59: 221–226.*
6. *L. Commin, M. Dumontb, R. Rotinata, F. Pierrona, J. E. Massec, L. Barrallierc, Influence of themicro structural changes and induced residual stresses on tensile properties of wrought magnesium alloy joints after FSW, Materials Science Engineering A. 2012; 551: 288–292.*

7. *S. Mironov, T. Onuma, Y. S. Sato, H. Kokawa, Microstructure evolution during friction- stir welding of AZ31 magnesium alloy, Acta Materials 2015; 120: 301–312.*
8. *Ananda Mohan Vemula, Evaluation of Microstructure and Mechanical Properties of Titanium alloy, International Journal of Mechanical and Production Engineering Research and Development. 2017; 7(3): 217-222.*
9. *P. K. Sahu, S. Pal, Multi-response optimization of process parameters in friction stir welded AM20 magnesium alloy by Taguchi grey relational analysis, Journal of Magnesium Alloy. 2015; 3: 36–46.*
10. *Shubhavardhan R N, Microstructure and Tensile Strength of Friction Stir Welding of Al-Cu, International Journal of Mechanical and Production Engineering Research and Development (IJMPERD), Volume 5, Issue 2, March - April 2015, pp. 41-50*
11. *Fusheng Pan, AnlianXu, Dean Deng, Junhua Ye, Xianquan Jiang, Aitao Tang and Yang Ran, Effects of friction stir welding on microstructure and mechanical properties of magnesium alloy Mg-5Al-3Sn, Materials and Design. 2016; 110: 266–274.*
12. *H. M. Rao, R. I. Rodriguez, J. B. Jordon, M. E. Barkey, Y. B. Guo, H. Badarinarayan, Friction stir spot welding of rare-earth containing ZEK120 magnesium alloy sheets, Materials and Design. 2014; 56: 750–754.*
13. *A. L. Xu, F. S. Pan, X. Q. Jiang, C. Li, Y. Ran, Microstructure and properties of friction stir welded Mg-1Al-xSn-0.3Mn magnesium alloys, Materials Science Forum. 2015; 816:349–355.*
14. *Ramanan. G, Edwin Raja Dhas, Ramachandran. M, Diju Samuel. G, Influence of activated carbon particles on microstructure and thermal analysis of metal matrix composites, Rasayan journal of chemistry. 2017;10: 375-384.*
15. *W. Guo, K. S. Wang, W. Wang, F. Wang, W. L. Wang, Influences of post-weld heat treatments on friction stir-welded AZ31B magnesium alloy joints, Rare Met. Mater. Eng. 2011; 40: 1075–1078.*
16. *S. Harosh, L. Miller, G. Levi, M. Bamberger, Microstructure and properties of Mg- 5.6%Sn-4.4%Zn-2.1%Al alloy, Journal of Materials Science. 2007; 42: 9983–9989.*
17. *Darwins. A. K, Satheesh. S, Effect of process parameters on microstructure and mechanical properties of friction stir welded ZE42 magnesium alloy, International Journal of Mechanical Engineering and Technology. 2017; 8(10): 484-492.*
18. *W. L. Xiao, S. S. Jia, L. D. Wang, Y. M. Wu, L. M. Wang, Effects of Sn content on the microstructure and mechanical properties of Mg-7Zn-5Al based alloys, Materials Science Engineering A. 2010; 527: 7002–7007.*
19. *Ramanan Gopalakrishnan, Edwin Raja Dhas John, Experimental investigation and multi response optimization of WEDM process of AA7075 metal matrix composites using particle swarm optimization, International journal of Intelligent Engineering and Systems. 2017;10(4): 166-176.*
20. *Maria Marinescua, Ana Emandia, Octavian G. Duliub, FT-IR, EPR and SEM–EDAX investigation of some accelerated aged painting binders, Vibrational Spectroscopy. 2014; 73: 127-134.*
21. *Diju Samuel. G, Edwin raja dhas. J, Ramanan. G, Ramachandran. M, Production and microstructure characterization of AA6061 matrix activated carbon particulate reinforced composite by friction stir casting method, Rasayan journal of chemistry. 2017; 10(3): 784-789.*
22. *Rajesh Prabha. N, Edwin Raja Dhas. J, Effect of TiC Effect of TiC and MoS_2 Reinforced aluminium Metal Matrix Composites on Microstructure and Thermo gravimetric Analysis, Rasayan journal of chemistry. 2017; 10(3):729-737.*